Trapped-Ion Quantum Logic with Global Radiation Fields

S. Weidt,[1] J. Randall,[1,2] S. C. Webster,[1] K. Lake,[1] A. E. Webb,[1] I. Cohen,[3] T. Navickas,[1] B. Lekitsch,[1] A. Retzker,[3] and W. K. Hensinger[1]

[1]*Department of Physics and Astronomy, University of Sussex, Brighton BN1 9QH, United Kingdom*
[2]*QOLS, Blackett Laboratory, Imperial College London, London SW7 2BW, United Kingdom*
[3]*Racah Institute of Physics, The Hebrew University of Jerusalem, Jerusalem 91904, Givat Ram, Israel*

(Received 21 September 2016; published 23 November 2016)

Trapped ions are a promising tool for building a large-scale quantum computer. However, the number of required radiation fields for the realization of quantum gates in any proposed ion-based architecture scales with the number of ions within the quantum computer, posing a major obstacle when imagining a device with millions of ions. Here, we present a fundamentally different approach for trapped-ion quantum computing where this detrimental scaling vanishes. The method is based on individually controlled voltages applied to each logic gate location to facilitate the actual gate operation analogous to a traditional transistor architecture within a classical computer processor. To demonstrate the key principle of this approach we implement a versatile quantum gate method based on long-wavelength radiation and use this method to generate a maximally entangled state of two quantum engineered clock qubits with fidelity 0.985(12). This quantum gate also constitutes a simple-to-implement tool for quantum metrology, sensing, and simulation.

DOI: 10.1103/PhysRevLett.117.220501

The control of the internal and external degrees of freedom of trapped ions using laser light has allowed unprecedented advances in the creation of multiparticle entangled states [1–4], quantum simulation [5–10], frequency standards [11], quantum sensing [12–14] and quantum logic [15,16]. A major goal is now to construct a large-scale quantum computer by scaling current systems up to a significantly larger number of ions [17–19]. The circuit-model approach for quantum information processing requires the realization of single qubit gates and a two-qubit entanglement operation [20]. The use of laser light for the implementation of these quantum logic operations has been extremely successful, with gate fidelities in the fault-tolerant regime having been achieved for single- [21,22] as well as two-qubit gates [22,23].

Instead of using laser light it is also possible to use long-wavelength radiation in the microwave and rf regime to implement quantum logic. Such fields are comparably simple to generate and highly stable and have already been used to implement single-qubit gates with errors of only 10^{-6}, far surpassing fault-tolerant thresholds [24]. Free-running long-wavelength radiation on its own is however not sufficient for the implementation of multiqubit gates, as it only weakly drives the ions' motion due to the vanishingly small Lamb-Dicke parameter. This drawback was first addressed in the seminal work by Mintert and Wunderlich in 2001 who showed that combining a static magnetic field gradient with externally applied long-wavelength radiation creates a sizable effective Lamb-Dicke parameter [25]. More recently, Ospelkaus *et al.* proposed using the oscillating magnetic field gradients experienced by an ion trapped in the near field of a microwave waveguide to perform multiqubit gates [26]. This scheme was subsequently used to perform the first microwave-based two-qubit gate by Ospelkaus *et al.* [27]. The fidelity of this particular gate scheme has recently been improved significantly [28], further demonstrating the potential of microwave-based quantum logic. The scheme requires ions to be trapped close to a surface incorporating the microwave waveguide and therefore the effects of motional heating must be more carefully considered. When scaling this approach, especially considering complicated electrode geometries such as X junctions, relevant individual microwave impedance matching for each gate zone across the whole architecture must be ensured. The addressing of individual ions would typically require the use of destructive interference incorporating all microwave fields applied within the range of the ion or other sophisticated methods [29,30].

The approach of using a static magnetic field gradient in conjunction with externally applied long-wavelength radiation is not subject to the above constraints (of course the effects of motional heating still need to be considered) and has also been used to implement a two-qubit gate between nearest as well as non-nearest neighbour ions [31]. In stark contrast to the work presented in this Letter, the first demonstration of using a static magnetic field gradient to implement a two-qubit gate [31] made use of an "undriven" magnetic gradient induced coupling. However, in this scheme the dominant source of noise is ambient magnetic field fluctuations as naturally occurring states with different magnetic moments must be used, ruling out the use of a so-called clock qubit. A promising approach to circumvent this drawback is to use "dressed states" [41–43] where one can quantum engineer an effective clock qubit that is highly protected from magnetic field fluctuations while maintaining a strong sensitivity to a static magnetic field gradient. They have already been used in single qubit operations [41,43]

 © 2016 American Physical Society

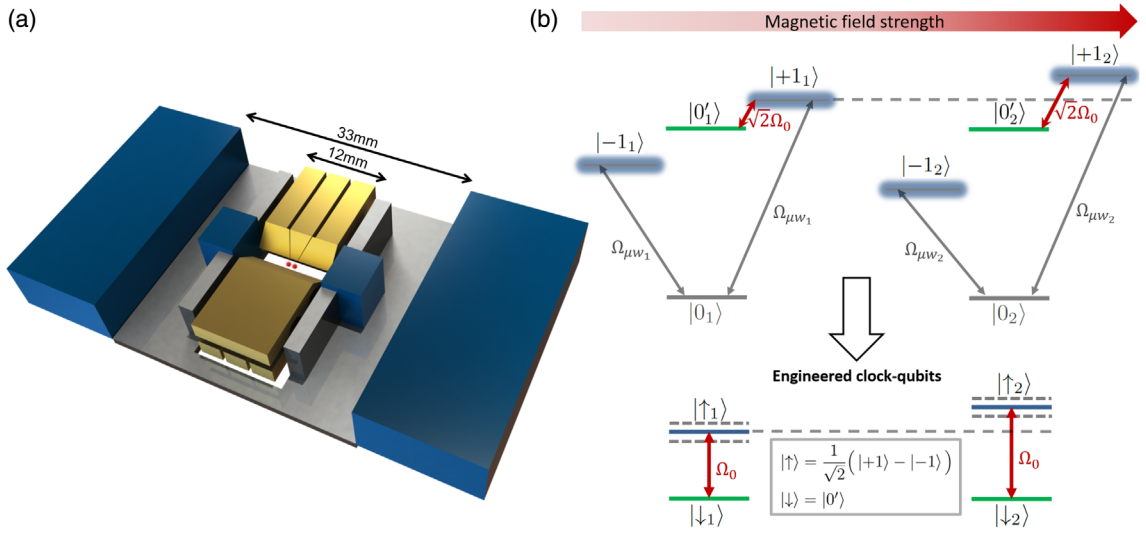

FIG. 1. (a) Schematic of the linear Paul trap (yellow) fitted with four permanent magnets (blue), arranged to create a strong magnetic field gradient along the trap axis. (b) Illustration of the $^2S_{1/2}$ ground-state hyperfine manifold of two $^{171}Yb^+$ ions, each being driven by two resonant microwave fields near 12.6 GHz with slightly unequal Rabi frequencies denoted by $\Omega_{\mu w_1}$ and $\Omega_{\mu w_2}$ (see the Supplemental Material [32]). The engineered clock qubit is formed of $|\uparrow\rangle = (|+1\rangle - |-1\rangle)/\sqrt{2}$ and $|\downarrow\rangle = |0'\rangle$, which can be manipulated using a rf field coupling $|0'\rangle$ and $|+1\rangle$ with Rabi frequency $\sqrt{2}\Omega_0$.

and to cool an ion close to its ground state of motion [44] and their use to implement a two-qubit gate would constitute a significant breakthrough for quantum computing with long-wavelength radiation.

Despite these successes, scaling these laser or long-wavelength radiation based operations to a much larger number of ions constitutes a tremendous challenge. This becomes particularly obvious when considering that a large-scale universal quantum computer, say of the size large enough to break RSA encoding, would require millions or even billions of qubits [19,45]. Gate operations need to be carried out in parallel for the quantum computer to work. The implication of this is that a large-scale quantum computer may require millions of spatially separated "gate zones" where quantum gates are executed. This results in the requirement of utilizing millions of laser or long-wavelength radiation fields for the implementation of quantum gates when considering all previous proposals to build a large-scale trapped-ion quantum computer [17–19,46]. This detrimental scaling between the number of ions and the required number of radiation fields constitutes a significant obstacle to scaling to the desired large system sizes.

In this work we remove this obstacle. We present a concept for trapped-ion quantum computing where parallel quantum gate operations in arbitrarily many selected gate zones can be executed using individually controlled voltages applied to each gate zone. Instead of millions of laser or long-wavelength radiation fields this simple approach only requires a handful of global radiation fields where the number of radiation fields only depends on the number of different types of quantum gates to be executed in parallel. This then provides a simple and powerful concept for quantum computing, which forms the core element within a wider engineering blueprint to build a large-scale microwave-based trapped-ion quantum computer [45]. A key element of our approach is the use of qubits that feature a widely tunable transition frequency while maintaining its protected nature with respect to ambient magnetic field fluctuations. Quantum-engineered clock qubits meet this requirement and therefore constitute an ideal system for this purpose. We demonstrate the key element of this approach by generating entanglement between microwave-based quantum-engineered clock qubits in a Mølmer-Sørensen-type interaction utilizing long-wavelength radiation and a static magnetic field gradient.

The two-qubit gate is performed on two $^{171}Yb^+$ ions in a Paul trap with an ion-electrode distance of 310 μm [47]. We place permanent magnets close to the ion trap with an ion-to-nearest-magnet distance of approximately 6 mm as shown in Fig. 1. This provides a static magnetic field gradient of 23.6(3) T/m, which is approximately constant across the ion string [48]. We slightly displace the ions from the magnetic field nil, which lifts the degeneracy of the $^2S_{1/2}$ $F = 1$ manifolds by 12.0 and 14.8 MHz for ions 1 and 2, respectively, and defines the internal-state quantization axis to lie along the trap axis. Laser light near resonant with the $^2S_{1/2} \leftrightarrow {}^2P_{1/2}$ transition is used for Doppler laser cooling and for initial state preparation as well as state detection. State-dependent fluorescence is collected on a photomultiplier tube, and the fluorescence measurements are normalized to remove preparation and detection errors (see the section entitled "Preparation and detection errors" in the Supplemental Material [32]).

To globally broadcast the required long-wavelength radiation we only require a standard off-the-shelf microwave horn and a three-turn rf-emitting copper coil placed outside the ultrahigh vacuum environment. We note that in a large-scale

architecture our approach utilizes submerged static currents incorporated into the microfabricated chip traps to give rise to the required static magnetic field gradients. The ion-surface distance requirement in this case is not very stringent. Simulations show magnetic field gradients in excess of 150 T/m with an ion-electrode distance of approximately 150 μm can be achieved, using realistic values of applied current that have already been applied to an ion trapping chip of this type [45]. Such a relatively large ion-electrode distance minimizes motional decoherence due to charge fluctuations from the electrode surface.

Instead of using a naturally occurring magnetic field sensitive qubit we quantum engineer a tunable highly noise-resilient "clocklike" qubit by first addressing each ion with a pair of microwave fields coupling the $|^2S_{1/2}, F = 0\rangle \equiv |0\rangle$ state with the $|^2S_{1/2}, F = 1, m_F = +1\rangle \equiv |+1\rangle$ and $|^2S_{1/2}, F = 1, m_F = -1\rangle \equiv |-1\rangle$ states (Fig. 1). In the appropriate interaction picture this results in three dressed states, including the well-protected state $|\uparrow\rangle = (|+1\rangle - |-1\rangle)/\sqrt{2}$ [41]. We combine this state with the intrinsically well-protected state $|^2S_{1/2}, F = 1, m_F = 0\rangle \equiv |\downarrow\rangle$ to obtain a quantum-engineered clock qubit $\{|\downarrow\rangle, |\uparrow\rangle\}$ (see the section entitled "Tunable quantum-engineered clock qubit" in the Supplemental Material [32]). Unlike a standard clock transition, which has a fixed transition frequency, the qubit transition frequency is tunable using a magnetic field, enabling individual qubit addressing with global radiation fields. This is a critical feature when viewed within the context of the novel approach for trapped-ion quantum computing outlined below. We prepare and detect the engineered clock qubit using the method developed by Randall *et al.* [49]. Arbitrary single qubit gates between states $|\downarrow\rangle$ and $|\uparrow\rangle$ are implemented using a rf field resonant with the $|\downarrow\rangle \leftrightarrow |+1\rangle$ transition [43]. The degeneracy in frequency between this and the $|\downarrow\rangle \leftrightarrow |-1\rangle$ transition is lifted by the second-order Zeeman shift. Using a Ramsey type experiment we measure the coherence time of this qubit to be 650 ms, significantly longer than the $\approx$1 ms coherence time of the bare state qubits that have so far been used for two-qubit gates with a static magnetic field gradient.

We create a maximally entangled state using a Mølmer-Sørensen type gate. The application of this gate to our qubit has been investigated in detail theoretically [41,50] and forms the basis of our experimental implementation. We implement the gate on the axial stretch mode with a frequency of $\nu_s = \sqrt{3}\nu_z = 2\pi \times 459.34(1)$ kHz, where ν_z is the axial center-of-mass mode frequency, giving an effective Lamb-Dicke parameter [25] $\eta_{\text{eff}} = z_0 \mu_B \partial_z B/\sqrt{2}\hbar\nu_s = 0.0041$, where $z_0 = \sqrt{\hbar/2m\nu_s}$. This mode is sideband cooled to $\bar{n} = 0.14(3)$ using a variant of the scheme described in Ref. [44] (see the section entitled "Sideband cooling" in the Supplemental Material [32]) before the internal states are prepared in the state $|\downarrow\downarrow\rangle$. A pair of rf fields is then applied to each ion with frequencies close to the red and blue sidebands (carrier Rabi frequency $\Omega_0 = 2\pi \times 45.4$ kHz). The frequencies are set to be symmetric about the carrier frequency, corresponding to detunings $\pm\nu_s \pm \delta$. The gate detuning δ is set to $\delta = 2\eta_{\text{eff}}\Omega_0 = 2\pi \times 370$ Hz in order that at time $t_g = 2\pi/\delta = 2.7$ ms the ions are ideally prepared in a maximally entangled spin state $|\Psi_{\phi_0}\rangle = (|\uparrow\uparrow\rangle + e^{i\phi_0}|\downarrow\downarrow\rangle)/\sqrt{2}$ (see the section entitled "Multiqubit gate" in the Supplemental Material [32]). Figure 2(a) shows the evolution of the spin state populations as a function of time. To measure the coherence of the entangled state, a carrier $\pi/2$ pulse is applied to each ion after the gate pulse. Figure 2(b) shows the parity $\Pi = P(\uparrow\uparrow) + P(\downarrow\downarrow) - P(\uparrow\downarrow) - P(\downarrow\uparrow)$ as a function of the phase ϕ of the $\pi/2$ pulse. The amplitude of the parity oscillation [Fig. 2(b)] along with the populations at t_g allows the fidelity of the obtained density matrix $\hat{\rho}$ with respect to the ideal outcome $|\Psi_{\phi_0}\rangle$ to be calculated using $\mathcal{F} = \langle\Psi_{\phi_0}|\hat{\rho}|\Psi_{\phi_0}\rangle = [P(\uparrow\uparrow) + P(\downarrow\downarrow)]/2 + A/2$ [3]. We measure the populations at t_g to be $P(\uparrow\uparrow) + P(\downarrow\downarrow) = 0.997(16)$ and a fit to the parity scan shown in Fig. 2(b) gives an amplitude of $A = 0.972(17)$. From this we extract a Bell state fidelity of $\mathcal{F} = 0.985(12)$.

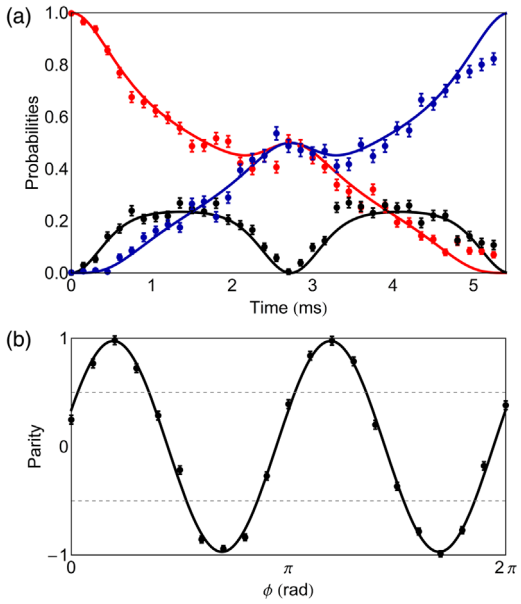

FIG. 2. (a) Populations $P(\uparrow\uparrow)$ (blue), $P(\downarrow\downarrow)$ (red), and $P(\uparrow\downarrow) + P(\downarrow\uparrow)$ (black) after preparing the ion spins in the state $|\downarrow\downarrow\rangle$ and applying the Mølmer-Sørensen fields for a variable time t. A maximally entangled state is formed at time $t_g = 2.7$ ms. Each data point is the average of 500 measurements and the solid lines are the predicted theoretical curves. (b) Parity $\Pi = P(\uparrow\uparrow) + P(\downarrow\downarrow) - P(\uparrow\downarrow) - P(\downarrow\uparrow)$ after applying the Mølmer-Sørensen interaction for a time t_g, followed by a $\pi/2$ pulse on each ion with variable phase ϕ. The signal oscillates as $\cos(2\phi)$, with an amplitude A that indicates the magnitude of the off-diagonal density matrix elements $|\rho_{\downarrow\downarrow,\uparrow\uparrow}|$ [3]. Each data point is the average of 800 measurements and the black line is a fit to the data.

The most significant contributions to the infidelity stem from the heating of the relevant vibrational mode of motion

(1×10^{-2}) used during the gate operation and depolarization of the qubit (3×10^{-3}). Both sources of error can be significantly reduced by increasing the gate speed using a larger static magnetic field gradient and by increasing Ω_0. The depolarization error can be further reduced by improving our microwave setup as a result of which a coherence time of seconds should be achievable as already demonstrated by Baumgart *et al.* [14]. Additional small sources of infidelity are discussed in the Supplemental Material [32].

Achieving gate fidelities that would enable fault-tolerant operation using global long-wavelength radiation can be realized either by the use of ion trap microchips or by a slight modification of our setup. By reducing the ion-to-nearest-magnet distance in a modified trap design to 2.4 mm, a magnetic field gradient of 150 T/m would result. This gives a large increase of the motional coupling strength, enabling a significant reduction of the error terms. Following a full numerical simulation of the system, a fidelity far above the relevant fault-tolerant threshold would result using already demonstrated parameters (see the section entitled "Further increasing the gate fidelity" in the Supplemental Material [32]).

We now describe how the gate method explained above gives rise to a highly efficient approach to quantum computing with trapped ions. In previously envisioned trapped-ion quantum computing architectures the number of radiation fields required for quantum gate implementation is strongly correlated with the number of ions used [17–19]. This constitutes a substantial challenge in the construction of a large-scale quantum computer, which may require the manipulation of millions or billions of ions. We will now outline an approach that completely removes this undesirable correlation where millions or billions of laser or long-wavelength radiation fields are replaced with only a handful of long-wavelength radiation fields.

Ions are located in individual gate zones that are contained within an array of X junctions as part of a microfabricated ion trap architecture (see Fig. 3). Currents applied locally to each gate zone create magnetic field gradients of approximately 150 T/m, to be used for entanglement generation. In order to select any arbitrary set of gate zones for single- or two-qubit gate execution, one simply shifts the position of the ion(s) within these zones axially with respect to the magnetic field gradient by an appropriate amount using local dc electrodes already used for ion transport within the ion trap array. In a magnetic field gradient, such shifts in the ion positions result in a variation of the local offset magnetic field. The transition frequency of the quantum-engineered clock qubit used in this work can be changed using such offset magnetic fields. This provides the ability to tune the quantum-engineered clock qubit into and out of resonance with globally applied long-wavelength radiation fields. Therefore, ions in any arbitrary zone can be tuned into resonance with a set of globally applied microwave and rf fields (of the sort used to implement the two-qubit gate presented in this Letter), providing parallel execution of

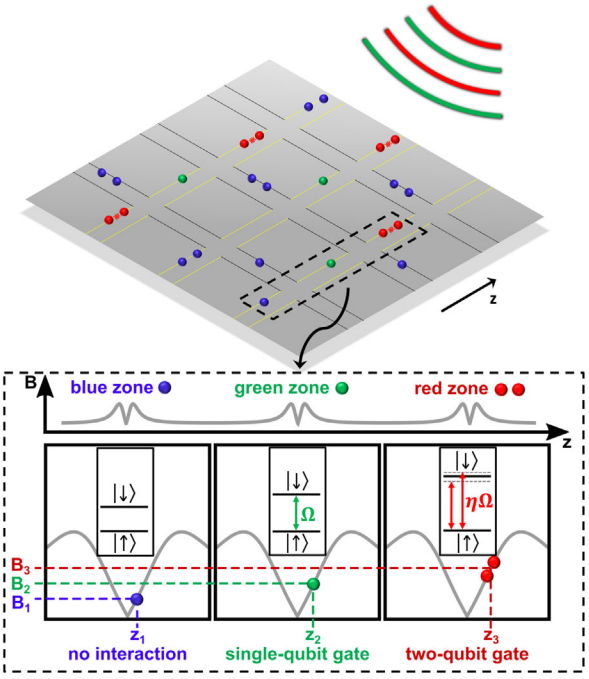

FIG. 3. Ions are confined in a two-dimensional X-junction surface trap architecture. Local dc electrodes are used to shift the center of the trapping potentials in the magnetic field gradient in order to tune a particular zone in resonance with a particular set of microwave and rf fields (illustrated in the dashed box). The ion displacements in the green (red) zones tune the respective ions into resonance with the global fields to realize single- (two-)qubit gates while no shift is applied to the blue zones, making all globally applied fields off resonant for ions located in these zones. Current-carrying wires (not shown for clarity) located below each gate zone (indicated by yellow lines) create a static magnetic field gradient local within each gate zone.

gates in relevant zones while all other zones on the architecture remain off resonant. Alternatively, instead of using the displacement of the ions to change the offset magnetic field, an offset magnetic field could be generated using additional local magnetic field coils located under each gate zone. Microwave horns and antennas located outside the vacuum system broadcast the required set of microwave and rf fields over the entire microchip or quantum computer architecture. Quantum operations are then applied in parallel to arbitrarily many sets of qubits with negligible cross talk (see the section entitled "Extension to a large-scale architecture" in the Supplemental Material [32]) using a small number of offset magnetic fields and associated sets of global microwave and rf fields, as shown in Fig. 3. Since the global fields are broadcast across the entire architecture, the number of required fields scales only with the number of different types of gates to be performed.

We have developed an efficient approach to quantum information processing with trapped ions. We proposed a method where gate operations within the trapped-ion quantum computer are facilitated by the application of

voltages to each logic gate location, analogous to transistors within a classical computer processor. Only a handful of global radiation fields, which are broadcasted across the entire quantum computer architecture, are required, no matter how many ions are used as part of the quantum computation. While there are still laser beams required for laser cooling, photoionization, repumping, and sympathetic cooling, these can be applied as global beams, so their number is not strongly correlated to the number of qubits and alignment and stability requirements are not very stringent. Besides describing the method, we have also reported the experimental demonstration of the key ingredient for this approach, namely, a new type of two-qubit entanglement gate utilizing long-wavelength radiation. Using this method we have created a maximally entangled state with fidelity close to the relevant fault-tolerant threshold. This method of creating high-fidelity entangled states may also have significant impact in areas other than quantum computing, owing to its simplicity and robustness. This simple-to-implement gate mechanism can be used in a large breadth of experiments in areas relying on the creation of entanglement such as quantum simulation, quantum sensing, and quantum metrology.

We thank Klaus Mølmer for helpful discussions and Eamon Standing for performing relevant magnetic field simulations. This work is supported by the U.K. Engineering and Physical Sciences Research Council [EP/G007276/1, the UK Quantum Technology hub for Networked Quantum Information Technologies (EP/M013243/1), the UK Quantum Technology hub for Sensors and Metrology (EP/M013294/1)], the European Commissions Seventh Framework Programme (FP7/2007-2013) under Grant Agreement No. 270843 (iQIT), the Army Research Laboratory under Cooperative Agreement No. W911NF-12-2-0072, U.S. Army Research Office Contract No. W911NF-14-2-0106, and the University of Sussex. A. R. acknowledges the support of the Israel Science Foundation (Grant No. 039-8823), the support of the European commission (STReP EQUAM Grant Agreement No. 323714), the Niedersachsen-Israeli Research Cooperation Program and DIP program (FO 703/2-1) and the support of the US Army Research Office under Contract No. W911NF-15-1-0250.

[1] R. Blatt and D. Wineland, Nature (London) **453**, 1008 (2008).
[2] H. Häffner, W. Hänsel, C. F. Roos, J. Benhelm, D. Chek-al-kar, M. Chwalla, T. Körber, U. D. Rapol, M. Riebe, P. O. Schmidt, C. Becher, O. Gühne, W. Dür, and R. Blatt, Nature (London) **438**, 643 (2005).
[3] C. A. Sacket, D. Kielpinski, B. E. King, C. Langer, V. Meyer, C. J. Myatt, M. Rowe, Q. A. Turchette, W. M. Itano, D. J. Wineland, and C. Monroe, Nature (London) **404**, 256 (2000).
[4] D. Leibfried, E. Knill, S. Seidlin, J. Britton, R. B. Blakestad, J. Chiaverini, D. B. Hume, W. M. Itano, J. D. Jost, C. Langer, R. Ozeri, R. Reichle, and D. J. Wineland, Nature (London) **438**, 639 (2005).
[5] R. Blatt and C. F. Roos, Nat. Phys. **8**, 277 (2012).
[6] A. Friedenauer, H. Schmitz, J. T. Glueckert, D. Porras, and T. Schaetz, Nat. Phys. **4**, 757 (2008).
[7] K. Kim, M.-S. Chang, S. Korenblit, R. Islam, E. E. Edwards, J. K. Freericks, G.-D. Lin, L.-M. Duan, and C. Monroe, Nature (London) **465**, 590 (2010).
[8] B. P. Lanyon *et al.*, Science **334**, 57 (2011).
[9] M. Johanning, A. F. Varón, and C. Wunderlich, J. Phys. B **42**, 154009 (2009).
[10] C. Schneider, D. Porras, and T. Schaetz, Rep. Prog. Phys. **75**, 024401 (2012).
[11] A. D. Ludlow, M. M. Boyd, J. Ye, E. Peik, and P. O. Schmidt, Rev. Mod. Phys. **87**, 637 (2015).
[12] S. Kotler, N. Akerman, Y. Glickman, A. Keselman, and R. Ozeri, Nature (London) **473**, 61 (2011).
[13] T. Pruttivarasin, M. Ramm, S. G. Porsev, I. I. Tupitsyn, M. S. Safronova, M. A. Hohensee, and H. Häffner, Nature (London) **517**, 592 (2015).
[14] I. Baumgart, J.-M. Cai, A. Retzker, M. B. Plenio, and C. Wunderlich, Phys. Rev. Lett. **116**, 240801 (2016).
[15] H. Häffner, C. F. Roos, and R. Blatt, Phys. Rep. **469**, 155 (2008).
[16] D. Leibfried, B. DeMarco, V. Meyer, D. Lucas, M. Barrett, J. Britton, W. M. Itano, B. Jelenkovic, C. Langer, T. Rosenband, and D. J. Wineland, Nature (London) **422**, 412 (2003).
[17] J. I. Cirac and P. Zoller, Nature (London) **404**, 579 (2000).
[18] D. Kielpinski, C. Monroe, and D. Wineland, Nature (London) **417**, 709 (2002).
[19] C. Monroe and J. Kim, Science **339**, 1164 (2013).
[20] M. A. Nielsen and I. L. Chuang, *Quantum Computation and Quantum Information* (Cambridge University Press, Cambridge, England, 2010).
[21] N. Akerman, N. Navon, S. Kotler, Y. Glickman, and R. Ozeri, New J. Phys., **17**, 113060 (2015).
[22] C. J. Ballance, T. P. Harty, N. M. Linke, M. A. Sepiol, and D. M. Lucas, Phys. Rev. Lett. **117**, 060504 (2016).
[23] J. P. Gaebler, T. R. Tan, Y. Lin, Y. Wan, R. Bowler, A. C. Keith, S. Glancy, K. Coakley, E. Knill, D. Leibfried, and D. J. Wineland, Phys. Rev. Lett. **117**, 060505 (2016).
[24] T. P. Harty, D. T. C. Allcock, C. J. Ballance, L. Guidoni, H. A. Janacek, N. M. Linke, D. N. Stacey, and D. M. Lucas, Phys. Rev. Lett. **113**, 220501 (2014).
[25] F. Mintert and C. Wunderlich, Phys. Rev. Lett. **87**, 257904 (2001).
[26] C. Ospelkaus, C. E. Langer, J. M. Amini, K. R. Brown, D. Leibfried, and D. J. Wineland, Phys. Rev. Lett. **101**, 090502 (2008).
[27] C. Ospelkaus, U. Warring, Y. Colombe, K. R. Brown, J. M. Amini, D. Leibfried, and D. J. Wineland, Nature (London) **476**, 181 (2011).
[28] T. P. Harty, M. A. Sepiol, D. T. C. Allcock, C. J. Ballance, J. E. Tarlton, and D. M. Lucas, Phys. Rev. Lett. **117**, 140501 (2016).

[29] U. Warring, C. Ospelkaus, Y. Colombe, R. Jördens, D. Leibfried, and D. J. Wineland, Phys. Rev. Lett. **110**, 173002 (2013).
[30] D. P. L. A. Craik, N. M. Linke, M. A. Sepiol, T. P. Harty, C. J. Ballance, D. N. Stacey, A. M. Steane, D. M. Lucas, and D. T. C. Allcock, arXiv:1601.02696.
[31] A. Khromova, C. Piltz, B. Scharfenberger, T. F. Gloger, M. Johanning, A. F. Varón, and C. Wunderlich, Phys. Rev. Lett. **108**, 220502 (2012).
[32] See Supplemental Material at http://link.aps.org/supplemental/10.1103/PhysRevLett.117.220501 for additional information on the experimental procedures, the gate mechanism and scaling considerations, which includes Refs. [33–40].
[33] J. Schrieffer and P. Wolff, Phys. Rev. **149**, 491 (1966).
[34] N. Aharon, M. Drewsen, and A. Retzker, Phys. Rev. Lett. **111**, 230507 (2013).
[35] A. Sørensen and K. Mølmer, Phys. Rev. Lett. **82**, 1971 (1999).
[36] A. Sørensen and K. Mølmer, Phys. Rev. A **62**, 022311 (2000).
[37] C. F. Roos, New J. Phys. **10**, 013002 (2008).
[38] L. Deslauriers, S. Olmschenk, D. Stick, W. K. Hensinger, J. Sterk, and C. Monroe, Phys. Rev. Lett. **97**, 103007 (2006).
[39] C. Piltz, B. Scharfenberger, A. Khromova, A. F. Varón, and C. Wunderlich, Phys. Rev. Lett. **110**, 200501 (2013).
[40] A. G. Fowler, M. Mariantoni, J. M. Martinis, and A. N. Cleland, Phys. Rev. A **86**, 032324 (2012).
[41] N. Timoney, I. Baumgart, M. Johanning, A. F. Varon, M. B. Plenio, A. Retzker, and C. Wunderlich, Nature (London) **476**, 185 (2011).
[42] T. R. Tan, J. P. Gaebler, R. Bowler, Y. Lin, J. D. Jost, D. Leibfried, and D. J. Wineland, Phys. Rev. Lett. **110**, 263002 (2013).
[43] S. C. Webster, S. Weidt, K. Lake, J. J. McLoughlin, and W. K. Hensinger, Phys. Rev. Lett. **111**, 140501 (2013).
[44] S. Weidt, J. Randall, S. C. Webster, E. D. Standing, A. Rodriguez, A. E. Webb, B. Lekitsch, and W. K. Hensinger, Phys. Rev. Lett. **115**, 013002 (2015).
[45] B. Lekitsch, S. Weidt, A. G. Fowler, K. Mølmer, S. J. Devitt, C. Wunderlich, and W. K. Hensinger, arXiv:1508.00420.
[46] C. Monroe, R. Raussendorf, A. Ruthven, K. R. Brown, P. Maunz, L.-M. Duan, and J. Kim, Phys. Rev. A **89**, 022317 (2014).
[47] J. J. McLoughlin, A. H. Nizamani, J. D. Siverns, R. C. Sterling, M. D. Hughes, B. Lekitsch, B. Stein, S. Weidt, and W. K. Hensinger, Phys. Rev. A **83**, 013406 (2011).
[48] K. Lake, S. Weidt, J. Randall, E. D. Standing, S. C. Webster, and W. K. Hensinger, Phys. Rev. A **91**, 012319 (2015).
[49] J. Randall, S. Weidt, E. D. Standing, K. Lake, S. C. Webster, D. F. Murgia, T. Navickas, K. Roth, and W. K. Hensinger, Phys. Rev. A **91**, 012322 (2015).
[50] G. Mikelsons, I. Cohen, A. Retzker, and M. B. Plenio, New J. Phys. **17**, 053032 (2015).